Jurnal Sains Farmasi & Klinis
p-ISSN: 2407-7062 | e-ISSN: 2442-5435
homepage: http://jsfk.ffarmasi.unand.ac.id
DOI : 10.25077/jsfk.11.1.67-79.2024

ORIGINAL ARTICLE J Sains Farm Klin 11(1):67–79 (April 2024) | DOI: 10.25077/jsfk.11.1.67-79.2024

Development of Oil Vehicle Screening Method for Bromo Acid Dye-Based Color-Changing Cosmetic Formulation

Eriwan Susanto[1], Juang Arwafa Cita[1], Ajeng Rana Wulan Sujilah[2], Satrialdi[2], Tri Suciati[2], & Yuda Prasetya Nugraha*[2]

[1]Research and Innovation Center, Paragon Technology and Innovation, Tangerang, Indonesia
[2]Department of Pharmaceutics, School of Pharmacy, Bandung Institute of Technology, Bandung, Indonesia

ABSTRACT: Bromo acid dye (Red 21) recently gained attention in the production of color-changing cosmetics. The critical aspect in the development of cosmetic products using this dye group is the compatibility of its oil vehicles. The compatibility of bromo acid dyes with oil vehicles is determined by several parameters such as the dye solubility in the oils, clarity of the mixture, and the ability to change color when the pH of the solution is adjusted to match the skin's pH. Therefore, this study conducted the compatibility study by examining the ability of 27 oil samples to dissolve Red 21. The ability of a vehicle to dissolve a compound is influenced by the polarity of the vehicle. Hence, a correlation was established between the relative polarity of oils and their ability to dissolve Red 21. The results showed that the water-oil interfacial tension was negatively correlated (r = -0.64) with Red 21 solubility in the oil. From this research, the water-oil interfacial tension represented the relative polarity of the oil and was considered sufficient to predict the compatibility of the oil with Red 21. In addition, hydrocarbon and silicone oils are not compatible with Red 21.

Keywords: **bromo acid; Red 21; oil vehicle; interfacial tension; solubility.**

Introduction

According to the report released by Fortune Business Insights in 2021, the global cosmetics market will grow by 44.2% in the period from 2021 to 2028. In addition, the cosmetics sector in Indonesia is seeing a growth rate of 7.5% from 2021 to 2027, positioning it as the fastest-growing market in Asia. It is projected to become one of the top five largest cosmetics markets globally [1]. As the cosmetics market expands, numerous novel advancements are being uncovered in the cosmetics industry. Various developments have been discovered in the field of cosmetics, ranging from delivery systems to new ingredients.

An emerging innovation trend in the cosmetics industry is color-changing cosmetics. These products have a transparent appearance but undergo an immediate color change when applied to the body. The strategy commonly employed in this type of cosmetic product involves the use of pH-sensitive coloring ingredients, such as bromo acid dyes. Bromo acid dye is an acid dye that is in the xanthine dye group [2]. Red 21 is one of the most frequently employed bromo acid dye in cosmetic formulations. Red 21 has three tautomeric forms that are determined by the local polarity and physical form of the dye. In principle, Red 21 has a transparent color when in its lactone form [3]. However, when it comes into contact with a moist application area and has a relatively acidic pH (4.0-7.0) [4] Red 21 will change to its monoanion or dianion form, which is capable of giving a yellowish into red color [3]. This dye also has the advantage to provide a fairly strong stain on the application area [5].

Cosmetic goods often contain several types of oils, including ester oils, hydrocarbon oils, silicone oils, fatty alcohols, triglycerides, and natural vegetable oils [6]. Each oil possesses distinct qualities, resulting in variations in its ability to dissolve and interact with bromo acid dyes. The process of creating cosmetics with bromo acid dyes typically involves challenges, one of which is locating a suitable oil vehicle [7]. The vehicle must possess the capability to dissolve and generate a slightly colored transparent blend, while producing the precise desired hue upon application. Therefore, it is necessary to conduct experiments to investigate the compatibility between oil vehicles and bromo acid dyes.

Article history
Received: 24 Jun 2023
Accepted: 28 Jun 2024
Published: 30 Jun 2024
Access this article

***Corresponding Author:** Yuda Prasetya Nugraha
Department of Pharmaceutics, School of Pharmacy, Bandung Institute of Technology, Bandung, Indonesia, 40132 | Email: yudapn@itb.ac.id

The ability of a solvent to dissolve a compound is influenced by its polarity [8]. The method of evaluating the relative polarity of an oil can be determined through several methods. One method that is considered less fastidious and gives a direct evaluation of oil polarity is through the determination of water-oil interfacial tension [9]. Based on this approach, through this research the author aims to develop a method to predict the compatibility of the oil vehicle with the Red 21 dye by making a correlation between the polarity of the oil vehicle, in this case by determining the interfacial tension and its ability to dissolve the Red 21 dye. The correlation determination aids in the future development of color-changing cosmetic goods.

Methods

Equipments and Materials

Materials that are used in this research are acetic acid glacial (99,7%), sodium acetate trihydrate, bromo acid dye Red 21 (CI 45380), Polyglyceryl-2 Triisostearate, Isononyl Isononanoate, Ethylhexyl Methoxycinnamate, Dicaprylyl Carbonate, Caprylyl Methicone, Isododecane, Octyldodecyl Stearoyl Stearate, Propylene Glycol Dicaprylate / Dicaprate, Hydrogenated Polyisobutene, Caprylic/Capric Triglyceride, Triethylhexanoin, Octyldodecanol, Cyclopentasiloxane, Dimethicone, Paraffinum Liquidum, Diisostearyl Malate, Argania Spinosa Kernel Oil, Squalane, Prunus Amygdalus Dulcis Oil, Phenyl Trimethicone, Olea Europaea (Olive) Fruit Oil, Ricinus Communis (Castor) Seed Oil, Pentaerythrityl Tetraisostearate, Octocrylene, and Isohexadecane (PT. Paragon Innovation and Technology Indonesia).

The equipment used in this research are analytical balance (Metler Toledo ME204), pycnometer 10 mL (Pyrex), viscometer (Brookfield DV type), tensiometer (Fisher Surface Tensiometer model 21), spectrophotometer UV-Vis (DU 7500i), water bath shaker (GFL 1092), ultrasonic bath, syringe 10 mL (OneMed Health Care), filter holder 13 mm (Sartorius Stedim Biotech), membrane filter (Sartorius Stedim Biotech), disposable syringe filter unit CA 13 mm 0,45 µm non-steril (Advantec), pH meter, and micropipette (Dragonlab).

Spesific Gravity Test

The spesific gravity of all the oil vehicles was measured with a 10 mL pycnometer at room temperature. The empty pycnometer (w_0) was weighed, then filled with distilled water and weighed again (w_1). After being emptied, it was then filled with oil and weighed once more (w_2). The specific gravity of the oil could be calculated by using the given formula:

$$\rho_o \quad \frac{w_2 \quad w_0}{w_1 \quad w_0} \quad 1\; g \;\; mL$$

Viscosity Test

The oil was tested using a Brookfield RV type viscometer with number 2 and 3 spindle needle, spinning at a speed from 10 to 100 RPM at room temperature.

Oil Relative Polarity Test

The relative polarity determination of 27 oil vehicles was carried out using the Du Nouy Ring method [10]. This determination is based on the interfacial tension value between oil and water. Oil vehicles or water are placed in a petri dish (based on their specific gravity, the one with the highest specific gravity is added first), and then the sample is placed on the sample table of the instrument. The sample table is raised until the ring part is submerged about 2-3 mm below the liquid surface. The second liquid with a lower specific gravity is added to the petri dish. Then, the sample table is slowly lowered until the ring pulls the liquid film to the bottommost part. At that moment, the value on the instrument will rise until it reaches its maximum value just before the ring leaves the bottommost liquid. This maximum value is finally taken as the reading value.

Solubility Test of Red 21 in Oil

The test was conducted in reference to [11] with modifications . A total of 25 mg of Red 21 dye was dissolved in 10 mL of oil sample, then stirred using a water bath shaker at a temperature of 28°C for 24 hours. Subsequently, the resulting solution from stirring was filtered using a non-sterile 0.45 µm cellulose acetate membrane filter to separate the saturated solution from the undissolved dye. The amount of the Red 21 dye dissolved in each oil sample was analyzed using UV-Vis spectrophotometry at the respective maximum absorption wavelength for each compound. In addition, a reference solution was prepared by dissolving 25 mg of Red 21 dye in 25 mL of oil sample, and then the reference solution was placed in an ultrasonic bath. The clarity and presence of undissolved dye precipitates in the reference solution were periodically visually checked. If the solution remained cloudy or there were still undissolved precipitates, additional volumes of oil were added, and then the reference solution was returned to the ultrasonic bath. Once the reference solution became clear and all precipitates were dissolved, the absorbance of the reference solution was measured

Table 1. Interpreting a correlation coefficient

Correlation Coefficient (r)	Interpretation
± 0,00 – 0,10	Negligible correlation
± 0,10 – 0,39	Weak correlation
± 0,40 – 0,69	Moderate correlation
± 0,70 – 0,89	Strong correlation
± 0,90 – 1,00	Very strong correlation

using UV-Vis spectrophotometry. The concentration of the saturated solution was then determined using the one-point method equation below:

$$C_s \quad \frac{C_r}{A_r} \quad A_s$$

C_s is the concentration of the saturated solution (%), C_r is the concentration of the reference solution (%), A_r is the absorbance of the reference solution, and A_s is the absorbance of the saturated solution.

Correlation between Relative Polarity of Oil and Solubility of Red 21 in Oil

The analysis used was descriptive statistical analysis. It was conducted on each measured parameter. The collected data was then grouped and categorized with the assistance of visualization tools from Visual Studio Code software. Subsequently, the correlation between the relative polarity of oils and their ability to dissolve Red 21 dye was determined. This analysis was performed using Python 3.10.5 with Jupyter Notebook in Visual Studio Code software. The libraries used were Pandas, SciPy, NumPy, Matplotlib, and Seaborn. The correlation between variables was determined by calculating the Pearson Correlation Coefficient (r) value. The interpretation of the correlation results can be seen in Table 1 [12].

The Effect of PH Changes on Color Formation

Certain amount of Red 21 was dissolved in each oil (0,02% w/w) and then filtered using a non-sterile 0.45 µm cellulose acetate membrane filter to separate the solution from the undissolved dye. Each solution was then photographed using a digital camera with standardized settings. Next, the photos were standardized using a color correction method based on a color chart image paper [13], and the color was segmented and quantified into RGB color codes. This analysis was performed using Python 4.9.0 with Jupyter Notebook on Anaconda software. The libraries used were NumPy, Matplotlib, and OpenCV. Afterwards, 500µL of acetate buffer (pH 5) was added to microcuvette and 500µL of Red 21 solution was added on top of the buffer solution while observing the color formation due to the pH changes.

Result and Discussion

First, 25 oil samples were classified by oil structure similarities into 7 groups of oils. Among these groups are

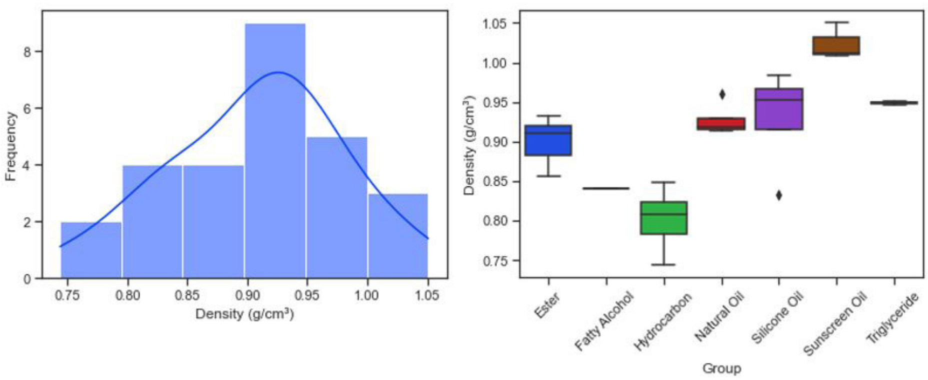

Figure 1. Spesific gravity distribution of the sample

Table 2. Classification of oil samples and solubility data of Red 21 in oil samples

Sample	Group	Code	Solubility (%)
Polyglyceryl-2 Triisostearate	Ester	ES-P2T	0,1326 ± 0,006
Isononyl Isononanoate	Ester	ES-INI	0,0387 ± 0,000
Dicaprylyl Carbonate	Ester	ES-DCC	0,0567 ± 0,002
Octyldodecyl Stearoyl Stearate	Ester	ES-OSS	0,0895 ± 0,006
Propylene Glycol Dicaprylate / Dicaprate	Ester	ES-PGD	0,1885 ± 0,001
Diisostearyl Malate	Ester	ES-DSM	-
Pentaerythrityl Tetraisostearate	Ester	ES-PET	0,0291 ± 0,001
Octyldodecanol	Fatty Alcohol	FA-ODD	0,0372 ± 0,001
Isododecane	Hydrocarbon	HC-IDD	-
Hydrogenated Polyisobutene	Hydrocarbon	HC-HPI	-
Paraffinum Liquidum	Hydrocarbon	HC-PLQ	-
Squalane	Hydrocarbon	HC-SQU	-
Isohexadecane	Hydrocarbon	HC-IHD	-
Argania Spinosa Kernel Oil	Natural Oil	NO-ARG	0,0457 ± 0,001
Prunus Amygdalus Dulcis Oil	Natural Oil	NO-PRU	0,0384 ± 0,003
Olea Europaea (Olive) Fruit Oil	Natural Oil	NO-OLE	0,0487 ± 0,004
Ricinus Communis (Castor) Seed Oil	Natural Oil	NO-RIC	0,1201 ± 0,002
Caprylyl Methicone	Silicone Oil	SO-CMC	-
Cyclopentasiloxane	Silicone Oil	SO-CPS	-
Dimethicone (Low viscosity)	Silicone Oil	SO-DMT-1	-
Dimethicone (High viscosity)	Silicone Oil	SO-DMT-2	-
Phenyl Trimethicone	Silicone Oil	SO-PTM	-
Ethylhexyl Methoxycinnamate (Low viscosity)	Sunscreen Oil	SC-EMC-1	-
Ethylhexyl Methoxycinnamate (High viscosity)	Sunscreen Oil	SC-EMC-2	1,7983 ± 0,031
Octocrylene	Sunscreen Oil	SC-OCL	0,0742 ± 0,004
Caprylic / Capric Triglyceride	Triglyceride	TG-CCT	0,1517 ± 0,006
Triethylhexanoin	Triglyceride	TG-THE	0,1091 ± 0,008

ester, fatty alcohol, hydrocarbon, natural oil, silicone oil, sunscreen oil, and triglyceride groups. Classification aims to identify the compatibility trends of each oil vehicles group with bromo acid dye, thereby facilitating the generalization of compatible oil carriers.The classification of oils can be seen in the following Table 2.

The data distribution of oil densities can be seen in Figure 1 (left). Based on the measurement results, the density of oil vehicles ranges from 0.7436 to 1.0505 g/cm^3, with an average density of all oil vehicles of 0.907 g/cm^3. Most oil vehicles have densities in the range of 0.90 to 0.95 g/cm^3. In Figure 1 (right), it can be observed that each group tends to have densities within specific ranges. The hydrocarbon group occupies the group of oils with the lowest density, while the sunscreen oil group occupies the group with the highest density.

The distribution of sample viscosities can be seen in Figure 2 (left). Based on the graph, it can be observed that the viscosity distribution of the samples ranges from 10.4 to 3896 cps. Therefore, viscosity is categorized into 3 categories : low viscosity represents samples with viscosities in the range of 10-100 cps, medium in the range of 100-1000 cps, and high viscosity represents samples with viscosities above 1000 cps as shown in Figure 2 (right). The categorization of viscosity aims to further investigate the correlation between viscosity parameters

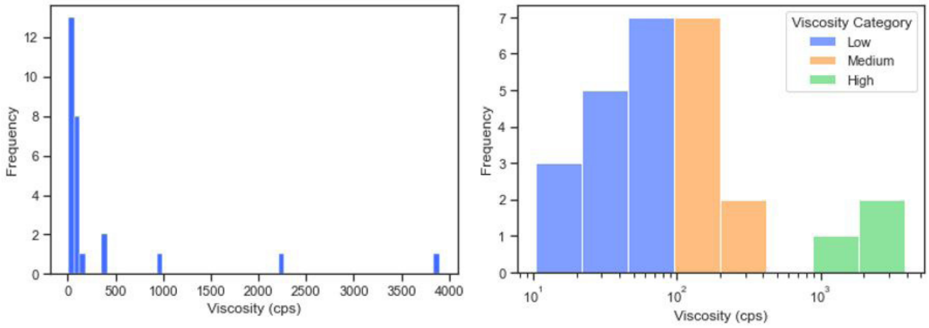

Figure 2. Viscosity distribution of the sample

and other parameters regarding the compatibility of oils with Red 21 dye.

Viscosity is a measure of the resistance of a fluid to flow when subjected to pressure. The higher the viscosity of a fluid, the higher its resistance [8]. The viscosity of a fluid is generally influenced by intermolecular forces as well as the shape and molecular structure of the fluid [14–16]. Based on its definition, viscosity can be understood as the result of forces that occur at the interface of various layers of a fluid. In other words, viscosity is the result of friction occurring between molecules. Intermolecular forces can play a role in the viscosity of a fluid because as intermolecular forces increase, the interaction between molecules in the fluid will become stronger, making it more difficult for molecules to flow and move [15]. Based on several previous studies, the structure and shape of molecules in a fluid can also affect its viscosity. According to the research done by Rodrigues et al., the length of the carbon chain, double bonds, and branching of a molecule can affect its viscosity. The longer the carbon chain, the fewer double bonds, and the fewer branches, the lower the viscosity of a fluid will be, and vice versa [16].

Based on Figure 3, it can be seen that most oil vehicles have viscosities ranging from 0 - 500 cps. However, only the sunscreen oil group has the highest viscosity. The viscosity range of ester oil group appears to be larger than the other groups, which may be due to the diversity of structures and shapes of oils within this group. There is one outlier in the ester oil group which is Polyglyceryl-2-Triisostearate oil. This may occur due to the high number of polar groups in this compound compared to other oil vehicles. Additionally, this oil also has 4 isostearate groups which are long-chain fatty acids. In the natural oil group, there is also an outlier from the castor oil vehicle. The

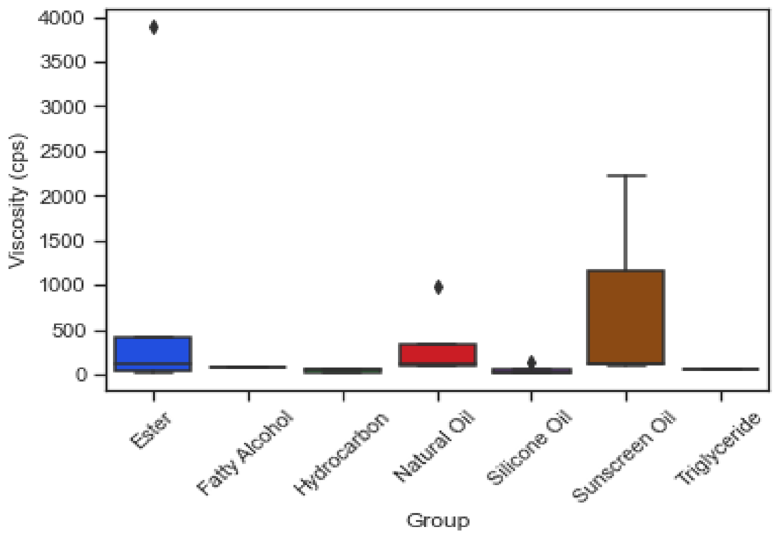

Figure 3. VViscosity distribution of the oil group

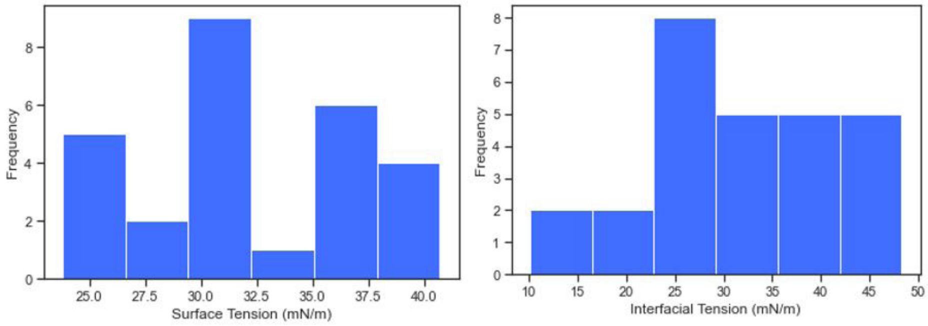

Figure 4. Relative polarity distribution of the sample

viscosity of castor oil differs from the other oil vehicles within its group possibly because castor oil contains Ricinoleic acid as its main component (70-90%) [17]. Ricinoleic acid is an unsaturated fatty acid with a hydroxyl group at C-12 in a cis position. The hydroxyl group at this position causes ricinoleic acid to have a stronger hydrogen bonding compared to other fatty acids [18].

In Figure 4 (left), it can be observed that the surface tension of the oils resulted in a range of 23.8 - 40.7 mN/m, with most oils having surface tensions in the range of 25 - 30 mN/m. Meanwhile, in Figure 4 (right) it can be seen that the oil-water interfacial tension of the samples ranges from 10.1 - 48.3 mN/m, with most interfacial tension values distributed above 30 mN/m.

Surface tension is the force per unit length required to balance the cohesive force possessed by a fluid at its surface, while interfacial tension is the force per unit length at the interface of two immiscible fluids [8]. At the oil-water interface, there is an adhesive force that can affect the value of oil-water interfacial tension in addition to the cohesive force of the two fluids. The adhesive force between the two fluids is influenced by interactions due to the molecular structure of both components. High adhesive forces cause the oil to spread on water due to the presence of polar groups in the oil, such as COOH or OH groups [8]. Unlike surface tension, the distribution of interfacial tension among the oil vehicles tends to be more diverse. This may be due to the many factors influencing interfacial tension ranging from molecular weight to the polar oil's ability to adsorb water on its surface [19].

Based on figure 5, the distribution of oil groups based on surface tension appears to be more diverse, where silicone oil is the group with the lowest surface tension and sunscreen oil is the group with the highest surface tension. The low surface tension of silicone oil is attributed to the interaction of its flexible backbone structure, linear shape, and minimal intermolecular interactions due to the absence of polar groups in the molecule [20,21]. Sunscreen oil is believed to have the highest surface tension due to its high cohesive forces between molecules. These cohesive forces result from the interactions between strong π bonds of conjugated double bonds within the oil group [22].

As shown in Table 2, 12 oil vehicles were unable to dissolve Red 21 dye, while 15 other oil vehicles were able to dissolve Red 21 dye, as indicated by the appearance of absorption peaks at wavelengths ranging from 450-575 nm. Bromo acid dyes are capable of imparting different colors when dissolved in various oil vehicles. The resulting

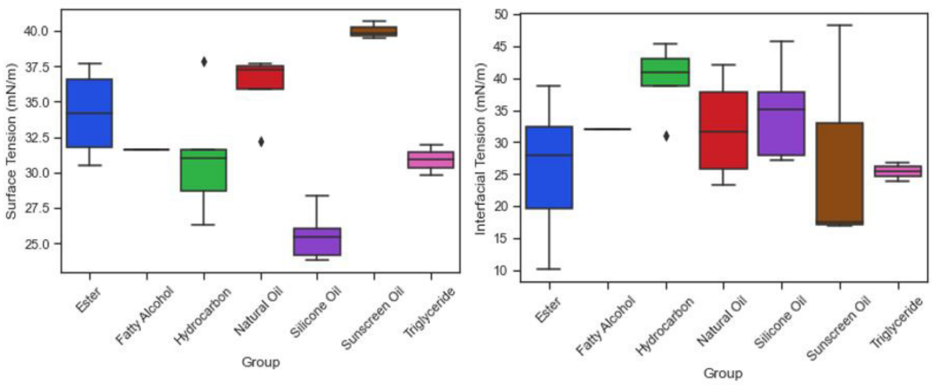

Figure 5. Relative polarity distribution of the oil group

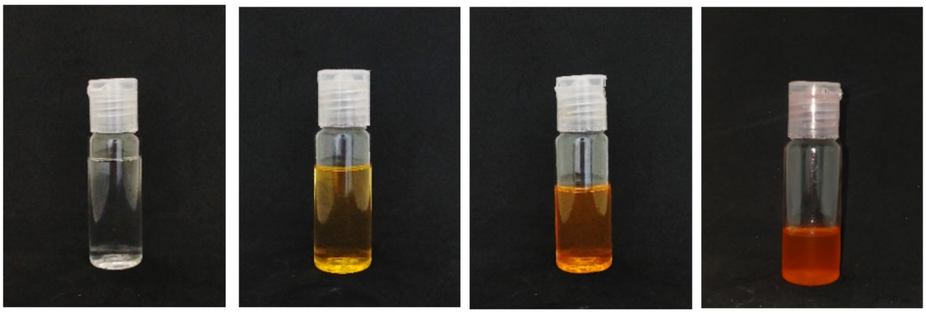

Figure 6. Various colors of Red 21 in samples

colors range from yellow to reddish-orange with varying color intensities. The light absorption produced falls within the wavelength range of 475 - 535 nm. These results are consistent with previous studies where bromo acid dyes were found to exhibit light absorption in the wavelength range of 450 - 575 nm [23–25]. Generally, the colors formed from the testing results are divided into 4 categories: colorless (undetected λmax in visible region), yellowish-orange (λmax 475 – 477 nm), orange (λmax 479 – 486 nm), and reddish-orange (λmax 535 nm), as shown in Figure 6.

In colorless solutions, no absorption peaks appear in the wavelength range of 450 – 575 nm, suggesting that the solubility of bromo acid dyes in those oils is very low or practically insoluble. The shift in maximum wavelength of bromo acid dyes is influenced by the polarity characteristics of the oil vehicles used [26]. The higher the polarity of the solvent used, the greater the bathochromic shift of the dye's λmax [27]. This may occur due to the strong interactions between oil vehicles, thereby weakening their ability to interact with the dye [28].

The determination of correlation between several variables begins with an initial screening of the overall data using a pairplot of Pearson correlation. Based on the results obtained, several parameters have been identified as candidates for further correlation analysis. As observed in Figure 7 (left), there is a tendency for samples with relatively high surface tension to have medium to high viscosity. A higher ranking of surface tension indicates a higher polarity of the sample [19]. Increased polarity of a fluid signifies an increase in intermolecular bonding of the fluid. Polar intermolecular interactions and large-sized molecules in the sample can provide more friction in the fluid, thus increasing its viscosity [15]. Through Figure 7 (right), it can be seen that there is no specific pattern exhibited by oil groups concerning surface tension or interfacial tension.

The Pearson correlation diagram shown in Figure 8 yields a value of r = -0.27, indicating a weak correlation between the ranking of surface tension and interfacial tension of oil vehicles. The negative value of the correlation aligns with the theory that as surface tension increases, the interfacial tension between oil and water decreases [19]. The weak relationship between these factors may be due to the fact that the interfacial tension values of the two immiscible liquid phases depend not only on the cohesive forces of each liquid but also on the specific interactions occurring between them [19]. Common

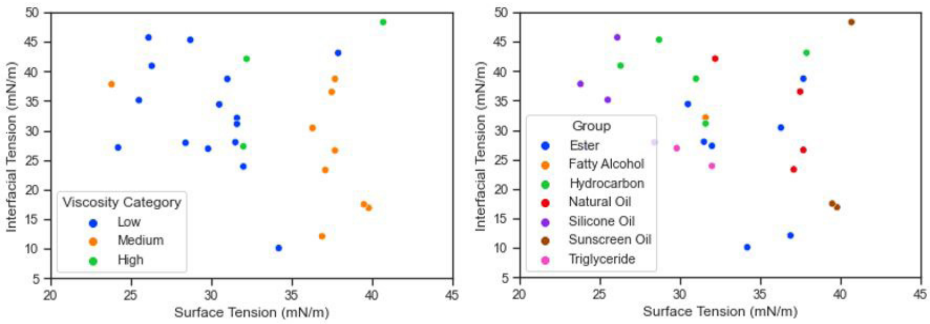

Figure 7. Correlation between surface tension and interfacial tension of samples

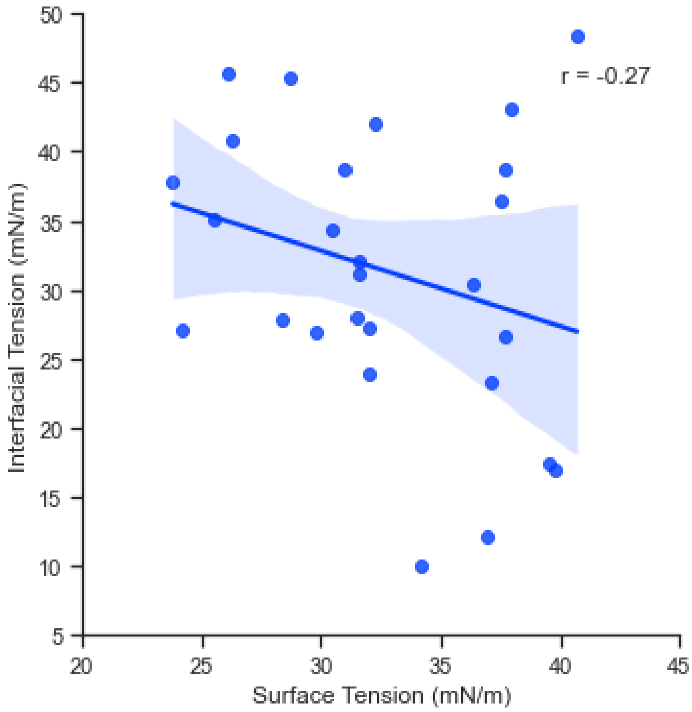

Figure 8. Pearson correlation diagram between surface tension and interfacial tension of samples

interactions occurring at the interface result from dipole-dipole and induced dipole interactions, dispersion forces, and interactions between electron acceptor and donor components of polar groups present in the oil [29,30].

Based on figure 9, it can be observed that silicone oil (purple dots) and hydrocarbon oils (green dots) completely lack the ability to dissolve bromo acid dyes. This is likely due to the highly hydrophobic nature of both oil groups and the absence of reactive groups in the oil vehicles capable of interacting with Red 21 dye [21]. Therefore, it can be concluded that silicone oil and hydrocarbon oil groups are not compatible with bromo acid (Red 21) dyes because they lack the ability to dissolve the dye.

In Figure 10 (left), it can be seen that oil groups with low surface tension or low polarity tend to be unable to dissolve bromo acid dyes. This aligns with previous research indicating that polar oils have better ability to dissolve bromo acid dyes compared to low polarity mineral oils [31]. Additionally, the correlation between surface tension and interfacial tension with dye solubility in the samples remains relatively weak, with a correlation of 0.32 for surface tension and -0.34 for interfacial tension. This may be due to the presence of outlier data from the SC-EMC-2 oil vehicle. This is suspected to be caused by strong π-π interactions between the phenyl groups of the oil vehicle and those of Red 21 dye [32]. Although belonging to the same group, the ability of the SC-OCL oil vehicle to dissolve Red 21 dye is not as strong as SC-EMC-2, as SC-OCL has electron-withdrawing substituents such as -CN groups in its structure, which

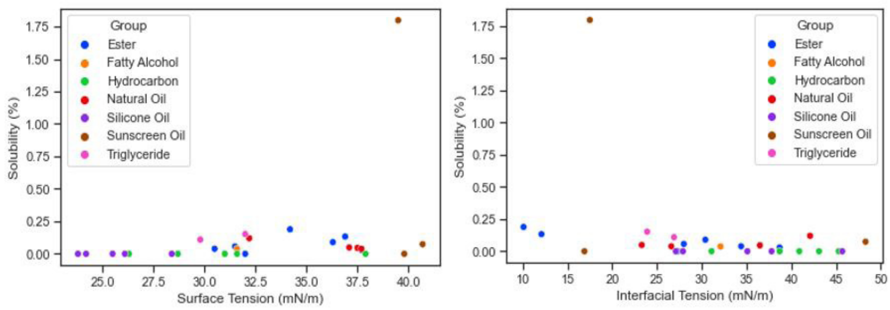

Figure 9. Correlation between surface tension and interfacial tension of samples

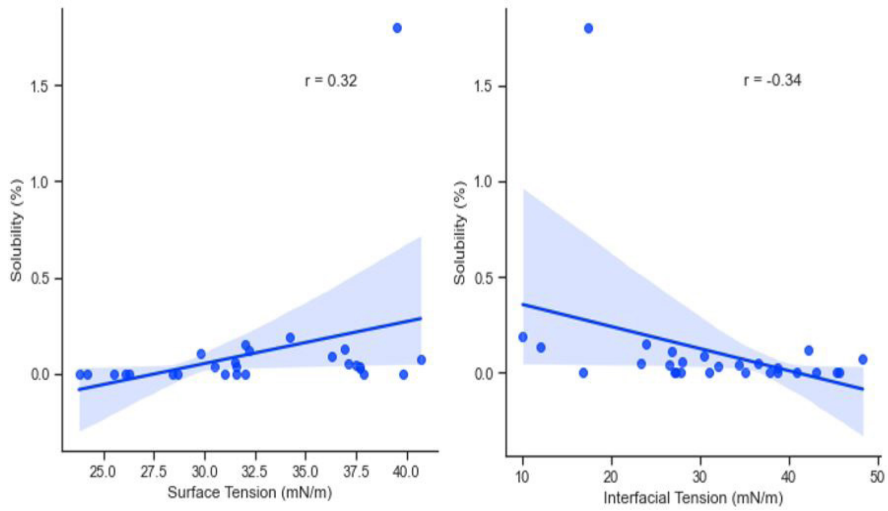

Figure 10. Pearson correlation diagram of sample relative polarity and Red 21 solubility (%)

can reduce electron density in the π system and thus decrease π-π intermolecular interactions [22,33]. Based on this approach, further correlation determination was conducted with the exclusion of solubility data from sunscreen oil group. Exclusion of the data from this oil group was due to the intermolecular interactions between the oil vehicles and the dye, which can act as predictors apart from the polar characteristics of the oil vehicles.

Subsequently, the correlation between the relative polarity of the oil vehicle and solubility was recalculated by removing data from the SC oil group. After removing data from the SC oil group, the correlation between interfacial tension and solubility showed an increase to a moderate correlation (r = -0.64), while the correlation between surface tension and solubility remained within the weak correlation range (r = 0.4). These results indicate that the interfacial tension value between the oil and water is more capable of representing the relative polarity value of an oil vehicle compared to its surface tension value and is considered sufficient to predict the compatibility of oil vehicles with Red 21 dye. Additionally, the correlation between oil-water interfacial tension and solubility is considered a moderate correlation because there are many other descriptors besides interfacial tension that can affect the polarity of a substance in its vehicle, such as the lipophilicity of the oil vehicle and dye [8].

Based on the results above, a trend was observed between interfacial tension and solubility of Red 21 in oil although the obtained correlation is still considered moderate. Afterwards, tests were conducted to observe

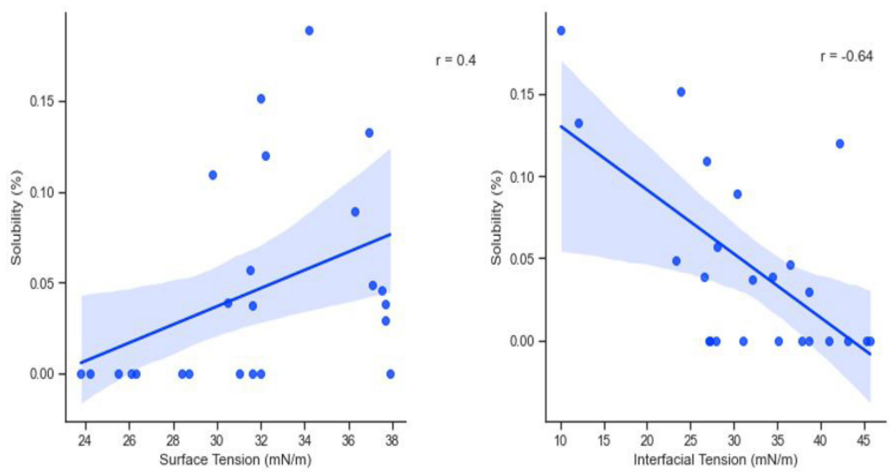

Figure 11. Pearson correlation diagram of relative polarity and Red 21 solubility (%) without SC group solubility data

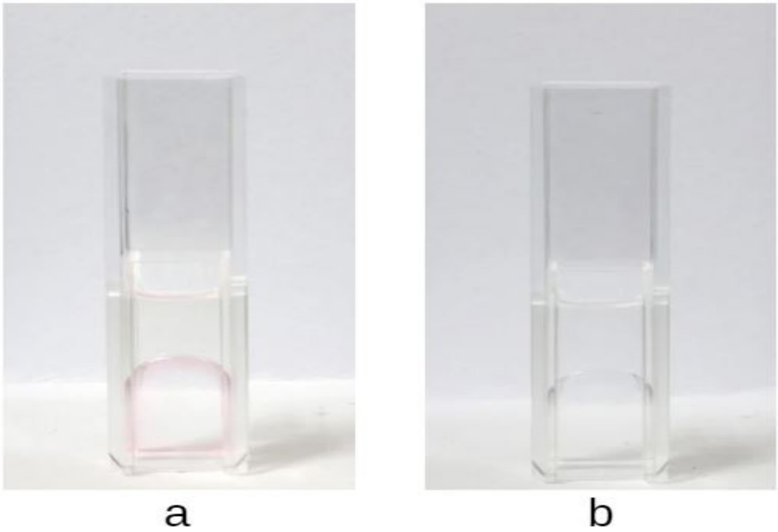

Figure 12. Color changing test results. (a) Positive result. (b) Negative result

color formation due to pH changes. In this testing method, several oils were able to elicit a color change in the aqueous phase. In other words, these oils were capable of carrying the Red 21 dye and releasing it into the aqueous phase. The differences in the color change response can be seen in Figure 12. The oils that were able to induce a color change in the aqueous phase include ES-PGD, TG-CCT, ES-P2T, NO-RIC, TG-THE, ES-OSS, SC-OCL, ES-DCC, NO-OLE, NO-ARG, ES-INI, NO-PRU, and FA-ODD. Interestingly, almost all the oils that could completely dissolve Red 21 at 0.02% were able to induce a color change in the aqueous phase. This indicates that the solubility of Red 21 in oil plays a crucial role in the color change. Exceptions occurred with ES-PET and SC-EMC-2, where SC-EMC-2 was an outlier in the correlation calculation between interfacial tension and the solubility of Red 21. There were no differences of the hue observed in the aqueous phase for each oil.

Each oil was able to produce different colors and intensities even when it has the same amount of Red 21 dye. Therefore, an analysis was conducted to compare the absorption spectra of each blank oil with the Red 21 dye solution in oil. According to the test results, it was found that several oils were able to influence the oil absorption

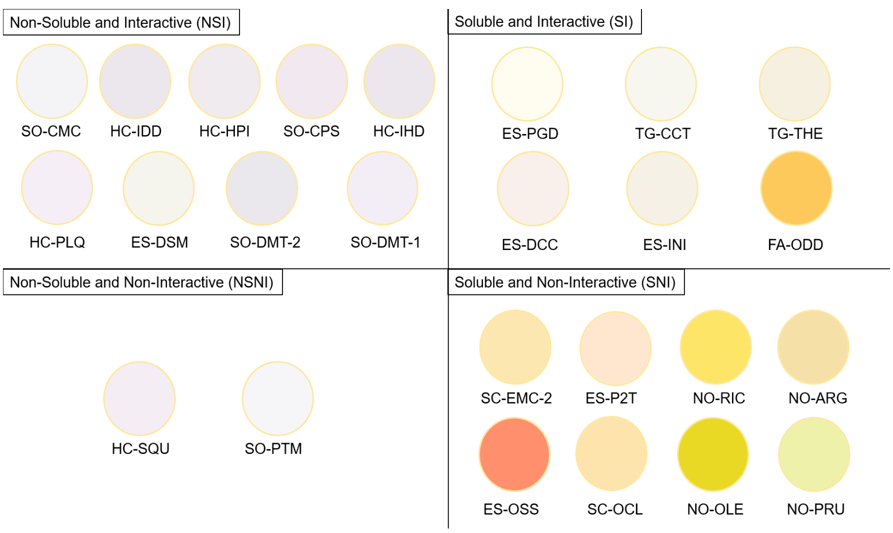

Figure 13. Classification of samples by Red 21 solubility and interaction

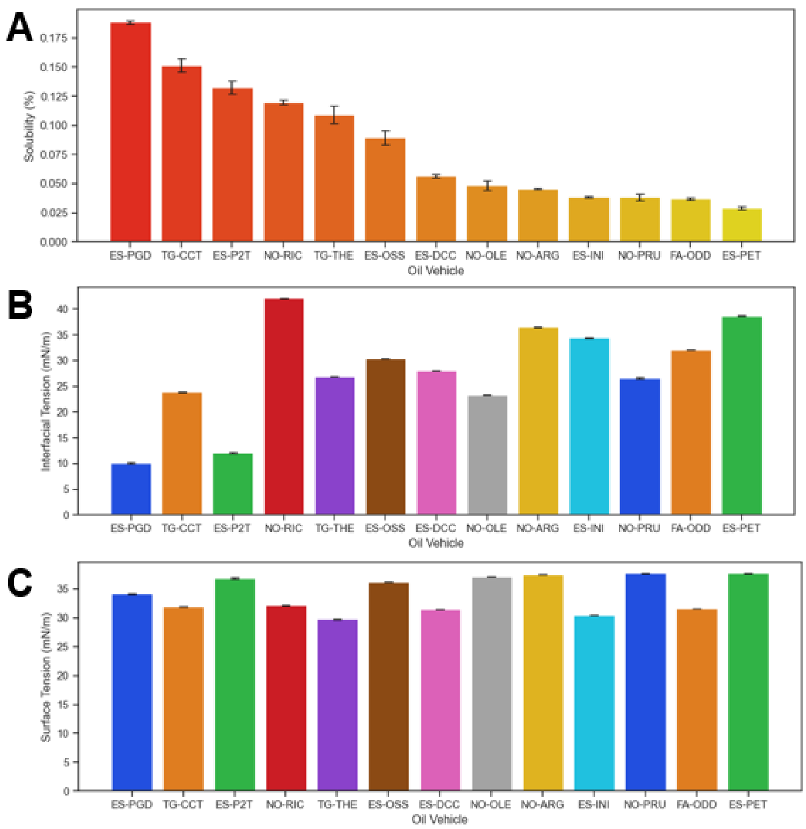

Figure 14. Correlation between surface tension and interfacial tension of samples

spectrum at the same peak wavelength. Oils that met this criterion were then classified as oils that interact with the Red 21 dye. Afterwards, the oils were classified into four groups: soluble and interactive (SI), soluble and non-interactive (SNI), non-soluble and interactive (NSI), and non-soluble and non-interactive (NSNI). The data of the oils based on this classification can be seen in Figure 13. There are several interesting points that can be observed from this classification. Most oils in the soluble and interactive group produced a color that tended to be faint and transparent, even though they contained the Red 21 dye. Therefore, oils in this group would be more desirable for making color-changing cosmetic preparations, especially for creating transparent formulations.

Data from the measurement results of Red 21 solubility, surface tension, and interfacial tension of oil vehicles deemed compatible with Red 21 through this method can be seen in Figure 14. The interfacial tension of oil vehicles generally rises as the oil's capacity to dissolve Red 21 diminishes, although no noticeable pattern is detected in the surface tension data for oil vehicles. A total of 13 oil vehicles deemed compatible with Red 21 dye by this method are ES-PGD, TG-CCT, ES-P2T, NO-RIC, TG-THE, ES-OSS, ES-DCC, NO-OLE, NO-ARG, ES-INI, NO-PRU, FA-ODD, and ES-PET. These 13 compatible oils are capable of dissolving Red 21 dye and providing a clear appearance. Additionally, the oil groups deemed incompatible with Red 21 dye are hydrocarbon oils and silicone oils. Ultimately, the oil vehicles deemed compatible with Red 21 dye through this method are ester oil, natural oil, fatty acid, and triglyceride groups, where these four oil groups are the most commonly encountered oils and have the simplest structures. The method of correlating interfacial tension with dye solubility is considered less suitable for use with sunscreen oil group oils because there are phenyl groups in these oils that cause strong π-π interactions with the dye, thus becoming a determinant of polarity apart from the influence of hydrogen bonding and molecular polarity of the oil vehicle [8].

Conclusion

The method used for determining the compatibility of oil vehicles with Red 21 dye is done by establishing the correlation between the oil-water interfacial tension and the solubility of Red 21 dye in the oil vehicles. This method is considered capable for predicting oil vehicle compatibility because a correlation coefficient value of -0.64 is obtained, which is classified as moderate correlation. The oil vehicle groups evaluated as incompatible with Red 21 dye through this method are hydrocarbon and silicone oil groups

Conflict of Interest

The authors have no conflicts of interest regarding this investigation.

Acknowledgement

This research was financially supported by PT. Paragon Technology and Innovation.

References

[1]. Ferdinand M, Ciptono WS. Indonesia's Cosmetics Industry Attractiveness, Competitiveness and Critical Success Factor Analysis. Jurnal Manajemen Teori dan Terapan | Journal of Theory and Applied Management. 2022;15(2):209–23. https://doi.org/10.20473/jmtt.v15i2.37451

[2]. Chatterjee S, Chatterjee S, Chatterjee BP, Das AR, Guha AK. Adsorption of a model anionic dye, eosin Y, from aqueous solution by chitosan hydrobeads. J Colloid Interface Sci. 2005;288(1):30–5. https://doi.org/10.1016/j.jcis.2005.02.055

[3]. Cooksey CJ. Quirks of dye nomenclature. 10. Eosin Y and its close relatives. Biotechnic and Histochemistry. 2018;93(3):211–9. https://doi.org/10.1080/10520295.2017.1413207

[4]. Lambers H, Piessens S, Bloem A, Pronk H, Finkel P, Household SL. Natural skin surface pH is on average below 5, which is beneficial for its resident flora. Vol. 28, International Journal of Cosmetic Science. 2006.

[5]. Rahman H. Utilization of Eosin Dye as An Ion Pairing Agent for Determination of Pharmaceuticals: A Brief Review. Int J Pharm Pharm Sci. 2017;9(12):1. https://doi.org/10.22159/ijpps.2017v9i12.21220

[6]. Harry RG. Harry's Cosmeticology. 9th ed. Meyer R, editor. Chemical Publishing Company; 2015.

[7]. Hoffmann F, Bayer A. Compatibility of dyes. Coloration Technology. 1988;18(1):56–64. https://doi.org/https://doi.org/10.1111/j.1478-4408.1988.tb00067.x

[8]. Martin AN, Sinko PJ. Martins Physical Pharmacy and Pharmaceutical Sciences,6th Edition. 6th ed. 2011.

[9]. El-Mahrab-Robert M, Rosilio V, Bolzinger MA, Chaminade P, Grossiord JL. Assessment of oil polarity: Comparison of evaluation methods. Int J Pharm. 2008;348(1–2):89–94. https://doi.org/10.1016/j.ijpharm.2007.07.027

[10]. Ebnesajjad S. Surface Tension and Its Measurement. In: Surface Treatment of Materials for Adhesive Bonding. Elsevier; 2014. p. 7–24. https://doi.org/10.1016/b978-0-323-26435-8.00002-2

[11]. Baka E, Comer JEA, Takács-Novák K. Study of equilibrium solubility measurement by saturation shake-flask method using hydrochlorothiazide as model compound. J Pharm Biomed Anal. 2008;46(2):335–41. https://doi.org/10.1016/j.jpba.2007.10.030

[12]. Schober P, Schwarte LA. Correlation coefficients: Appropriate use and interpretation. Anesth Analg. 2018;126(5):1763–8. https://doi.org/10.1213/ANE.0000000000002864

[13]. Sinthanayothin C, Bholsithi W, Wongwaen N. Color Correction on Digital Image Based on Reference Color Charts Surrounding Object. 2016;

[14]. Panwar P, Schweissinger E, Maier S, Hilf S, Sirak S, Martini A. Effect of polymer structure and chemistry on viscosity index, thickening efficiency, and traction coefficient of lubricants. J Mol Liq. 2022;359. https://doi.org/10.1016/j.molliq.2022.119215

[15]. Ruihan W, Ji-Hong C, Huizinga J. On the Relationship Between Viscosity and Surface Tension. J Emerg Investig. 2014;

[16]. Rodrigues J, Cardoso F, Lachter E, Estevao L, Lima E, Nascimento RS. Correlating Chemical Structure and Physical Properties of Vegetable Oil Esters. J Am Oil Chem Soc. 2006;83(4):353–7.

[17]. Buist PH. Unsaturated Fatty Acids. In: Comprehensive Natural Products II. 2010. p. 5–33. https://doi.org/10.1016/B978-008045382-8.00720-6

[18]. Parekh VJ, Rathod VK, Pandit AB. Substrate Hydrolysis: Methods, Mechanism, and Industrial Applications of Substrate Hydrolysis. In: Comprehensive Biotechnology, Second Edition. Elsevier Inc.; 2011. p. 104–18. https://doi.org/10.1016/B978-0-08-088504-9.00094-5

[19]. Kronberg B, Holmberg K. Surface Chemistry of Surfactants and Polymers [Internet]. 2014. Available from: www.wiley.com.

[20]. Grundke K, Michel S, Knispel G, Grundler A. Wettability of silicone and polyether impression materials: Characterization by surface tension and contact angle measurements. Colloids Surf A Physicochem Eng Asp. 2008;317(1–3):598–609. https://doi.org/10.1016/j.colsurfa.2007.11.046

[21]. Huber P, Wacker WK. Silicone Fluids: Synthesis, Properties Applications and. Journal of Synthetic Lubrication. 1986;3(2):105–20. https://doi.org/https://doi.org/10.1002/jsl.3000030204

[22]. Kushwaha K, Yu L, Stranius K, Singh SK, Hultmark S, Iqbal MN, et al. A Record Chromophore Density in High-Entropy Liquids of Two Low-Melting Perylenes: A New Strategy for Liquid Chromophores. Advanced Science. 2019;6(4). https://doi.org/10.1002/advs.201801650

[23]. Cheng D-X, Wang S-H, Liu W-J. Studies on the Spectra of 4,5-Dibromofluorescein with Proteins and its Analytical Application.

[24]. Khalid Hamood Al-Behadili W, Jawad YM, Hasan HJ. Study the Effect of PH on Absorption and Fluorescence Spectra of Eosin Y Dye in Ethanol. Asian Journal of Green Chemistry. 2023;7(3):163–74. https://doi.org/10.22034/ajgc.2023.393691.1381

[25]. Slyusareva E, Sizykh A, Tyagi A, Penzkofer A. Spectral and photophysical properties of fluorone dyes in bio-related films and methanol. J Photochem Photobiol A Chem. 2009;208(2–3):131–40. https://doi.org/10.1016/j.jphotochem.2009.09.006

[26]. Bosveli A, Montagnon T, Kalaitzakis D, Vassilikogiannakis G. Eosin: a versatile organic dye whose synthetic uses keep expanding. Vol. 19, Organic and Biomolecular Chemistry. Royal Society of Chemistry; 2021. p. 3303–17. https://doi.org/10.1039/d1ob00301a

[27]. Airinei A, Homocianu M, Dorohoi DO. Changes induced by solvent polarity in electronic absorption spectra of some azo disperse dyes. J Mol Liq. 2010;157(1):13–7. https://doi.org/10.1016/j.molliq.2010.07.011

[28]. Rauf MA, Soliman AA, Khattab M. Solvent effect on the spectral properties of Neutral Red. Chem Cent J. 2008;2(1). https://doi.org/10.1186/1752-153X-2-19

[29]. Marmur A, Valal D. Correlating interfacial tensions with surface tensions: A gibbsian approach. Langmuir. 2010;26(8):5568–75. https://doi.org/10.1021/la9038478

[30]. Miadonye A, Irwin DJG, Amadu M. Effect of Polar Hydrocarbon Contents on Oil-Water Interfacial Tension and Implications for Recent Observations in Smart Water Flooding Oil Recovery Schemes. ACS Omega. 2023;8(10):9086–100. https://doi.org/10.1021/acsomega.2c04698

[31]. Rieger M. Harry's Cosmeticology: 8th Edition, Volume 2. 8th ed. Rieger M, editor. Vol. 2. Chemical Publishing Company; 2000.

[32]. West A. Intermolecular Forces and Solvation. In: Interface Science and Technology. Elsevier B.V.; 2017. p. 49–130. https://doi.org/10.1016/B978-0-12-801970-2.00002-1

[33]. Kumar M, Thakur A, Mandal UK, Thakur A, Bhatia A. Foam-Based Drug Delivery: A Newer Approach for Pharmaceutical Dosage Form. Vol. 23, AAPS PharmSciTech. Springer Science and Business Media Deutschland GmbH; 2022. https://doi.org/10.1208/s12249-022-02390-x.